Economic Dispatch with Heavy Loading and Maximum Loading Identification Using Convex Relaxation of AC OPF

Abdullah Alassaf
Electrical Engineering Department
University of South Florida, USA
University of Hail, KSA
Email: Alassaf@mail.usf.edu

Lingling Fan
Electrical Engineering Department
University of South Florida, USA
Email: Linglingfan@usf.edu

***Abstract*— The objective of this paper is to explore two engineering applications of convex relaxation of AC OPF: (i) to conduct economic dispatch at heavy loading conditions; and (ii) to identify the system's loading limit. The conventional AC OPF formulation solved by interior point method has difficulty to converge when the system is reaching its loading limit due to the singularity of the Jacobian matrix. Existing methods to identify loading limits include continuous power flow (CPF) method. For CPF, the direction of power transfer has to be identified first. Then, a PV nose is obtained and the maximum loading level is at the nose point. Using convex relaxation of alternating current optimal power flow (AC OPF), we will not encounter singularity issues. In this paper, we will formulate a semi-definite programming (SDP) relaxation of AC OPF-based optimization problems to conduct economic dispatch and loading limit identification. Advantages of SDP OPF over MATPOWER are demonstrated. Further, loading limits identified by SDP OPF are compared with those found using the CPF method of MATPOWER. Our research indicates that two methods will lead to the same solutions for the tested systems.**

I. Introduction

This paper exploits an engineering application of convex relation of AC OPF. The particular relaxation used in this paper is the SDP relaxation [1], [2]. Conventional AC OPF is a nonconvex program and is usually solved by the interior-point method. MATPOWER [3] is one such software package for AC OPF using interior-point method. The conventional power flow equations are listed as the equality constraints in AC OPF. When evoking interior-point method-based solvers, those power flow equations have to be solved.

For power flow equations, Newton-Raphson method has a convergence issue when the system loading reaches its limit. Similarly, when the system is reaching its limit, AC OPF also has a convergence issue and the interior-point method-based solver does not give a solution.

An advantage of SDP relaxation is that the power flow equations are no longer in terms of voltage magnitude and angles. Instead, power flow equations are linear to the elements of a positive semi-definite (PSD) matrix. This new expression makes the convergence issue disappear.

Thus, we can employ SDP relaxation of AC OPF to identify loading limit or to find economic dispatch of generators when the system is close to its loading limit. In addition, when the system is over its loading limit, SDP relaxation will indicate that there is no feasible solution.

Using SDP relaxation of AC OPF and second order cone programming relaxation of AC OPF to identify loading limit has been addressed in [4], [5].

In this paper, we investigate the two optimization problem formulation based on SDP OPF to investigate both economic dispatch under heavy loading and loading limit identification. Comparison with MATPOWER will be given to demonstrate the advantages of SDP OPF.

This paper is organized as follows. In Section II, we give AC OPF formulation in the conventional and SDP relaxation forms. In Section III, we show the advantage of semi-definite programming using CVX over nonlinear programming using MATPOWER in solving optimal power flow problems. In Section IV, the maximum loading level identification is carried by SDP OPF and MATPOWER's runcpf function. Conclusion of this paper in found in Section V.

II. AC OPF

The objective functions and the constraints of power system depend on the applications that need to be optimized. The essential active power objectives and constraints of a general OPF problem are given in Table I [6].

TABLE I
Essential Active Power OPF Objectives and Constraints [6]

Objectives	Constraints
• Economic dispatch (minimum cost losses, MW generation, or transmission losses) • Environmental dispatch • Maximum power transfer	• Generator output in MW • Operating limits of MW and MVAr • MW and MVAr interchanges

A. Mathematical AC OPF Formulation

The typical AC OPF formulation is to minimize the generation cost while considering the system's physical operation limits. For a system with n buses, the parameters and decision variables are listed as follows.

- $V_k = V_{dk} + jV_{qk}$: The voltage phasor in rectangular coordinates.
- $Y_{kj} = G_{kj} + jB_{kj}$: The admittance between Bus k and Bus j.
- P_k and Q_k are the active and reactive injected power at Bus k, respectively.
- P_{Gk} and Q_{Gk} are the active and reactive generated power at Bus k, respectively.
- P_{Dk} and Q_{Dk} are the active and reactive demand power at Bus k, respectively.
- Subscripts $_{\max}$ and $_{\min}$ notate maximum and minimum limits, respectively.
- α_k , β_k, and γ_k are the constant, linear and quadratic fuel cost coefficients of unit k.

The conventional AC OPF formulation for minimizing the generation cost of a system is shown in (1) and (2).

$$\min \quad F_{cost}(P_{Gk}) = \sum_{k\epsilon G}(\alpha_k + \beta_k P_{Gk} + \gamma_k P_{Gk}^2) \tag{1}$$

subject to:

$$P_k = V_{dk}\left(\sum_{j=1}^{n}(V_{dj}G_{k,j} - V_{qj}B_{k,j})\right) + V_{qk}\left(\sum_{j=1}^{n}(V_{qj}G_{k,j} - V_{dj}B_{k,j})\right) \tag{2a}$$

$$Q_k = V_{qk}\left(\sum_{j=1}^{n}(V_{dj}G_{k,j} - V_{qj}B_{k,j})\right) - V_{dk}\left(\sum_{j=1}^{n}(V_{qj}G_{k,j} + V_{dj}B_{k,j})\right) \tag{2b}$$

$$P_k - P_{Gk} + P_{Dk} = 0 \tag{2c}$$

$$Q_k - Q_{Gk} + Q_{Dk} = 0 \tag{2d}$$

$$V_{k,\min} \leq V_k \leq V_{k,\max} \tag{2e}$$

$$P_{Gk,\min} \leq P_{Gk} \leq P_{Gk,\max} \tag{2f}$$

$$Q_{Gk,\min} \leq Q_{Gk} \leq Q_{Gk,\max} \tag{2g}$$

B. Mathematical AC OPF Formulation in SDP Form

In this subsection, AC OPF formulation is set to be in the SDP form [2]. e_1, e_2, e_3, . . . , and e_n are the standard basis vectors in $\mathbb{R}^n$. $\mathbf{M_1}$, $\mathbf{M_2}$, $\mathbf{M_3}$, . . . , and $\mathbf{M_n}$ are the standard basis matrices. k is the bus index. $\Re$ and $\Im$ are the real and imaginary components, respectively.

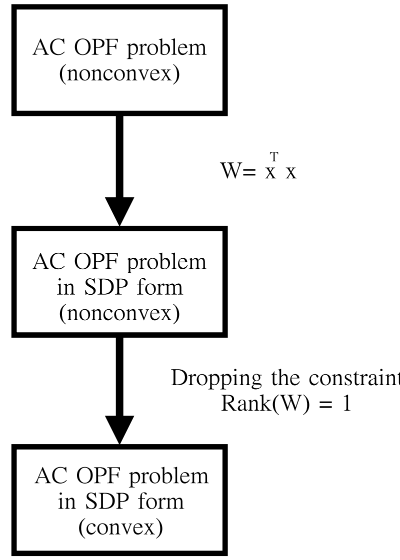

Fig. 1. The Convexification Process.

$$Y_k = e_k e_k^T Y \tag{3a}$$

$$\mathbf{Y}_k = \frac{1}{2}\begin{bmatrix}\Re(Y_k + Y_k^T) & \Im(Y_k^T - Y_k)\\ \Im(Y_k - Y_k^T) & \Re(Y_k + Y_k^T)\end{bmatrix} \tag{3b}$$

$$\tilde{\mathbf{Y}}_k = -\frac{1}{2}\begin{bmatrix}\Im(Y_k + Y_k^T) & \Re(Y_k - Y_k^T)\\ \Re(Y_k^T - Y_k) & \Im(Y_k + Y_k^T)\end{bmatrix} \tag{3c}$$

$$\mathbf{M}_k = \begin{bmatrix}e_k e_k^T & 0\\ 0 & e_k e_k^T\end{bmatrix} \tag{3d}$$

$$\mathbf{X} = [\Re(V)^T \quad \Im(V)^T]^T \tag{3e}$$

$$W = XX^T \tag{3f}$$

$$\text{Rank}(W) = 1 \tag{3g}$$

$$W \succeq 0 \tag{3h}$$

$$P_k = \text{Trace}\{Y_k W\} \tag{3i}$$

$$Q_k = \text{Trace}\{\tilde{Y}_k W\} \tag{3j}$$

$$P_k^{\min} - P_{D_k} \leq \text{Trace}\{Y_k W\} \leq P_k^{\max} - P_{D_k} \tag{3k}$$

$$Q_k^{\min} - Q_{D_k} \leq \text{Trace}\{\tilde{Y}_k W\} \leq Q_k^{\max} - Q_{D_k} \tag{3l}$$

$$(V_k^{\min})^2 \leq \text{Trace}\{\mathbf{M}_k W\} \leq (V_k^{\max})^2 \tag{3m}$$

The bus reference angle is set to be 0^{o} by forcing V_{qk} to be 0. This is obtained by the following equations [7].

$$\mathbf{N}_k = \begin{bmatrix}0 & 0\\ 0 & e_k e_k^T\end{bmatrix} \tag{4a}$$

$$\text{Trace}\{N_1 W\} = 0 \tag{4b}$$

The convexification of AC OPF form is realized by dropping the rank constraint, Rank$(W) = 1$. The convexification process is shown in Fig. 1.

III. Economic Dispatch Under Heaving Loading

In this section, we go through study cases and solve them using MATPOWER for conventional AC OPF and CVX

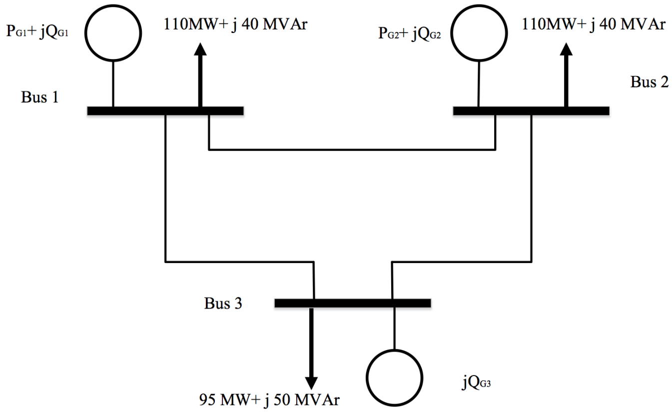

Fig. 2. Three-Bus System Case Study [9]

[8] with the SDPT3 solver for SDP OPF. MATPOWER solves the original nonlinear programming based AC OPF constraints in (2). On the other hand, CVX toolbox with the SDPT3 solver solves the SDP relaxation of AC OPF constraints in (3). We start with a 3-bus system, then we conduct 6- and 14- bus systems. We have tested larger scale systems up to 118-bus system, however, they are not shown in this paper due to space restrictions.

A. Three-Bus System

This system is adopted from [9]. The system is shown in Fig. 2. The optimal solution of the system using MATPOWER, which applies Interior Point Method in nonlinear programming, is shown in Table II. CVX optimal solution, which is based on semidefinite programming, is found in Table III. We can see that the two solutions match from Table II and Table III.

TABLE II
THREE-BUS SYSTEM MATPOWER SOLUTION

Bus	$\|V\|$(p.u.)	δ (degrees)	P_G(MW)	Q_G(MVAr)
Bus 1	1.1	0	128.46	42.52
Bus 2	1.1	9.001	188.22	49.13
Bus 3	1.1	-11.641	0	70.29
Total Generation Cost = 5694.54 $ /hour				

TABLE III
THREE-BUS SYSTEM CVX SOLUTION

Bus	$\|V\|$(p.u.)	δ (degrees)	P_G(MW)	Q_G(MVAr)
Bus 1	1.1	0.0031	128.4570	42.5181
Bus 2	1.1	9.0006	188.2194	49.1240
Bus 3	1.1	-11.6410	0	70.2930
Total Generation Cost = 5694.5366 $ /hour				

Next, the system gets tested with very high power demands. The power demands are shown in Table IV. MATPOWR could not solve the problem, it does not converge after 20 iterations. On the other hand, CVX solves the problem, the solution is given in Table V. As the load at

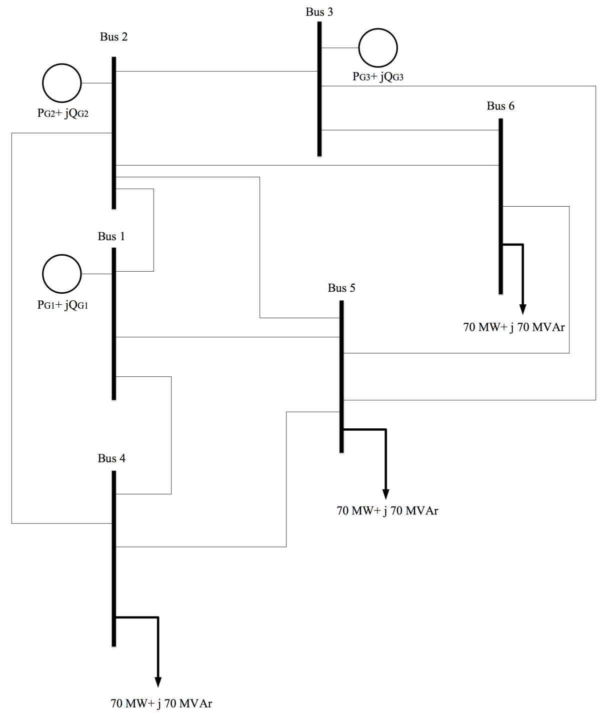

Fig. 3. Six-Bus System Case Study [10]

Bus 3 increases to 329.76, CVX can not solve the problem because the solution is in the infeasible area, which is beyond the AC OPF problem relaxation. In this case, infeasibility means the system is exceeding the operation limits. Thus, SDP OPF gives the ability to depict the system operation at its physical limits.

TABLE IV
THREE-BUS SYSTEM WITH POWER DEMANDS

Bus	P_D(MW)	Q_D(MVAr)
Bus 1	300	150
Bus 2	315	150
Bus 3	329.73	150

TABLE V
THREE-BUS SYSTEM CVX SOLUTION

Bus	$\|V\|$(p.u.)	δ (degrees)	P_G(MW)	Q_G(MVAr)
Bus 1	1.1	0.0011	499.7572	302.9615
Bus 2	1.1	4.3729	491.5208	300.5785
Bus 3	1.1	-83.8065	0	503.7369
Total Generation Cost = 51,097.3 $ /hour				

B. Six-Bus System

The 6-Bus system is taken from [10], it is shown in Fig. 3. The optimal solution of the system using CVX matches MATPOWER, and it is shown in Table VI.

Again, the power demands dramatically increase to prove that CVX can solve the problem when it operates at its

TABLE VI

SIX-BUS SYSTEM CVX AND MATPOWER SOLUTION

Bus	$\|V\|$(p.u.)	δ (degrees)	P_G(MW)	Q_G(MVAr)
Bus 1	1.050	0	50	35.33
Bus 2	1.050	-0.45	89.63	55.88
Bus 3	1.070	-0.545	77.07	84.88
Bus 4	0.987	-2.051	0	0
Bus 5	0.985	-2.745	0	0
Bus 6	1.005	-2.555	0	0
Total Generation Cost = 3126.36 $ /hour				

physical limits, and MATPOWER cannot. The demand loads are found in Table VII, and the solution is shown in Table VIII.

TABLE VII

SIX-BUS SYSTEM WITH INCREASING POWER DEMANDS ON BUS 4, 5 AND 6

Bus	P_D(MW)	Q_D(MVAr)
Bus 4	150	84
Bus 5	100.5	90
Bus 6	101	80

TABLE VIII

SIX-BUS SYSTEM CVX SOLUTION

Bus	$\|V\|$(p.u.)	δ (degrees)	P_G(MW)	Q_G(MVAr)
Bus 1	1.0500	0.0825	107.0510	51.7093
Bus 2	1.0500	-1.8654	116.4908	99.9985
Bus 3	1.0700	-0.1343	144.9349	99.9979
Bus 4	0.9500	-5.6386	0	0
Bus 5	0.9526	-4.5743	0	0
Bus 6	0.9883	-3.8457	0	0
Total Generation Cost = 5013.52 $ /hour				

C. IEEE 14-Bus System

Now, we solve IEEE 14-Bus system [11], shown in Fig. 4. We do a little adjustment on the system, and that is we ignore the compensation on bus 9. The reason is that we show the effect of reactive power on maximum loading level on the bus in the following section. We use CVX and MATPOWER to solve the system. Both methods give the same optimal solution that is given in Table IX.

If the active power load at bus 14 only increases to 79.657 MW, MATPOWER cannot solve the problem because it does not converge. CVX, on the other hand, gives the solution in Table X. Beyond this value, CVX shows that the solution is infeasible.

IV. IDENTIFYING MAXIMUM LOAD LEVEL

As the bus demand load increases, the voltage and the frequency decrease for both the bus and the system [12]. Control systems can be used to restore them, however, there are certain limitations of the system to handle power demands. In this section, we investigate the maximum loading level on bus and determine the bus voltage while the maximum load occurs. In our examination, we release the power generation

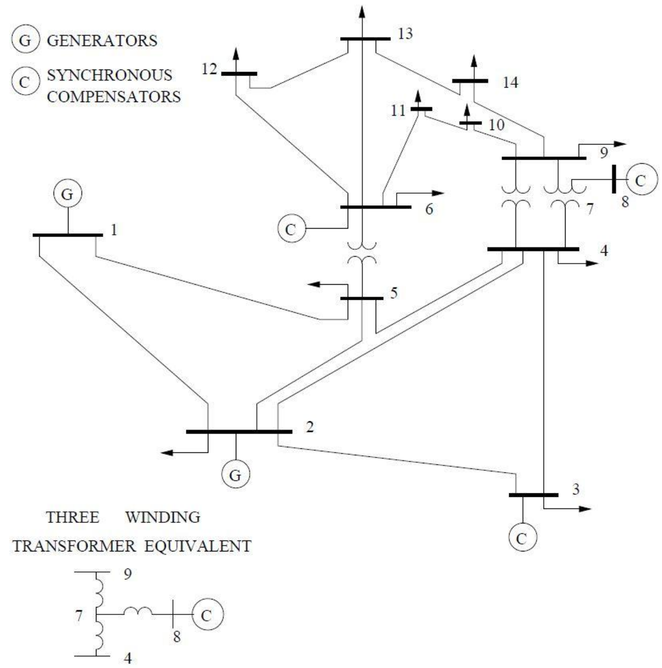

Fig. 4. IEEE 14-Bus System Case Study [11]

TABLE IX

IEEE 14-BUS SYSTEM CVX AND MATPOWER SOLUTION

Bus	$\|V\|$(p.u.)	δ (degrees)	P_G(MW)	Q_G(MVAr)
Bus 1	1.0600	0	194.2590	0
Bus 2	1.0418	-4.0410	36.7089	32.0250
Bus 3	1.0159	-9.9429	28.7408	26.6046
Bus 4	1.0099	-8.5832	0	0
Bus 5	1.0125	-7.3788	0	0
Bus 6	1.0501	-10.2621	0	14.8189
Bus 7	1.0332	-11.1178	0	0
Bus 8	1.0600	-10.3331	8.7387	16.1913
Bus 9	1.0179	-12.9168	0	0
Bus 10	1.0160	-13.1979	0	0
Bus 11	1.0293	-13.1433	0	0
Bus 12	1.0336	-13.6974	0	0
Bus 13	1.0276	-13.7176	0	0
Bus 14	1.0035	-14.3278	0	0
Total Generation Cost = 8088.22 $ /hour				

TABLE X

IEEE 14-BUS SYSTEM CVX SOLUTION

Bus	$\|V\|$(p.u.)	δ (degrees)	P_G(MW)	Q_G(MVAr)
Bus 1	1.0600	-0.0081	37.8290	0
Bus 2	1.0600	-0.2932	105.4574	17.2126
Bus 3	1.0600	-2.7409	83.3948	35.5711
Bus 4	1.0302	-3.3345	0	0
Bus 5	1.0287	-3.1624	0	0
Bus 6	1.0600	-9.1917	13.0089	24.0000
Bus 7	1.0332	-2.3175	0	0
Bus 8	1.0600	6.3088	93.2573	23.1423
Bus 9	1.0175	-7.3617	0	0
Bus 10	1.0176	-7.9776	0	0
Bus 11	1.0352	-8.6963	0	0
Bus 12	1.0360	-10.6632	0	0
Bus 13	1.0184	-11.1546	0	0
Bus 14	0.9400	-16.0732	0	0

and the bus voltage limits of the tested bus. By these steps, we find the maximum demand power on the tested bus, as well as the voltage at that level. Identifying the maximum loading level is equivalent to determining the voltage stability margins. That is, increasing the load above the maximum limit causes voltage collapse and system instability. We also show that the ability of loading increases as the tested bus reactive power raises. We go through the same study cases in the previous section. The solution is obtained by using CVX.

A. Maximum Loading Level Formulation

The following are the objective function, which is maximizing load on the tested bus, and the physical system constraints.

$$\max \qquad P_{Di} \tag{5}$$

Subject to:

$$(2)$$

Note: the voltage constraint on the tested bus is relaxed.

B. Three-Bus System

Starting with ignoring the synchronous condenser on bus 3, we find the bus voltage and the maximum power loading using (2) and (5), the result is found in Table XI. As bus 3 is compensated by a synchronous condenser with a value of 50 MVAr, the bus voltage and the maximum power loading are enhanced. The result with compensation is also shown in Table XI.

TABLE XI
THREE-BUS SYSTEM MAXIMUM LOADING LEVEL

Bus	$\|V\|$(p.u.)	δ^o	P_D(MW)	Compensation
Bus 3	0.7153	-63.0728	113.3347	Q_{G3} = 0 MVAr
Bus 3	0.8465	-69.9686	141.7333	Q_{G3} = 50 MVAr

The solutions from SDP OPF are compared with continuation method using MATPOWER CPF. The PV curves are shown in Fig. 5. As bus 3 is compensated with 50 MVAr, the nose, critical, point gets upper-right shifted. The reason is that the loading level and the voltage become higher. The two methods lead to the same results.

C. Six-Bus System

In this system, the investigated buses are 4, 5, and 6. We have examined each bus separately. Then, every bus is compensated with a synchronous condenser with a value of 20 MVAr. The results of maximizing the load level on each bus with and without compensation are shown in Table XII.

The comparison between optimization and continuation methods on the 6-bus system is applied on bus 4 without compensation. Bus 4 PV curve is shown Fig. 6. The two methods lead to the same results of 487 MW as Bus 4's loading limit.

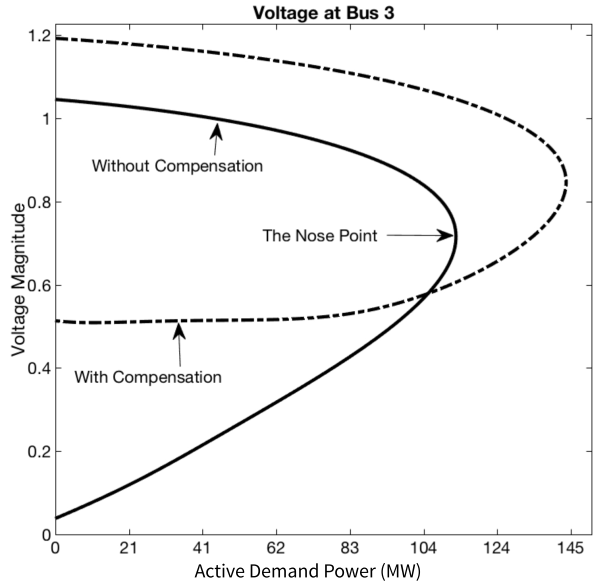

Fig. 5. Bus 3 PV Curve

TABLE XII
SIX-BUS SYSTEM MAXIMUM LOADING LEVEL

Bus	$\|V\|$(p.u.)	δ (degrees)	P_D(MW)	Compensation
Bus 4	0.6735	-56.9789	486.7798	Q_{G4} = 0 MVAr
Bus 4	0.6842	-58.1005	497.6326	Q_{G4} = 20 MVAr
Bus 5	0.6646	-63.4751	427.5265	Q_{G5} = 0 MVAr
Bus 5	0.6770	-64.8659	438.0877	Q_{G5} = 20 MVAr
Bus 6	0.7879	-56.7647	450.0843	Q_{G6} = 0 MVAr
Bus 6	0.8370	-87.5602	453.3528	Q_{G6} = 20 MVAr

D. IEEE 14-Bus System

The PQ buses in IEEE 14-Bus System are 4, 5, 7, 9, 10, 11, 12, 13, and 14. By repeating the same procedure, each bus is tested alone, the solution is found in Table XIII. Afterward, a synchronous condenser of values of 19, 30, 50, 100, 150 and 200 MVAr are step-by-step added to bus 9 only to prove that the maximum loading level increases as the reactive power raises. The solution of bus 9 maximum loading level with compensation is found in Table XIII.

By using bus 9 of the 14-bus system to compare optimization and continuation methods. The PV curve of bus 9, with Q_{G9} = 0 MVAr, is shown Fig. 7. Both methods show that for Bus 9, 352 MW is the loading limit.

V. CONCLUSION

This paper gives a review of applying SDP AC OPF to find economic dispatch at heavy loading condition and identify loading limits. Relaxation of AC OPF problem in SDP form gives an exact or an approximate global solution without iterations. We show that the AC OPF problem in SDP form can be solved using CVX. We test the CVX on various power system types. Then, we compare the solution with MATPOWER, which applies the interior point method in nonlinear programming. We find the solutions match each other. Moreover, CVX has the ability to give a solution of a

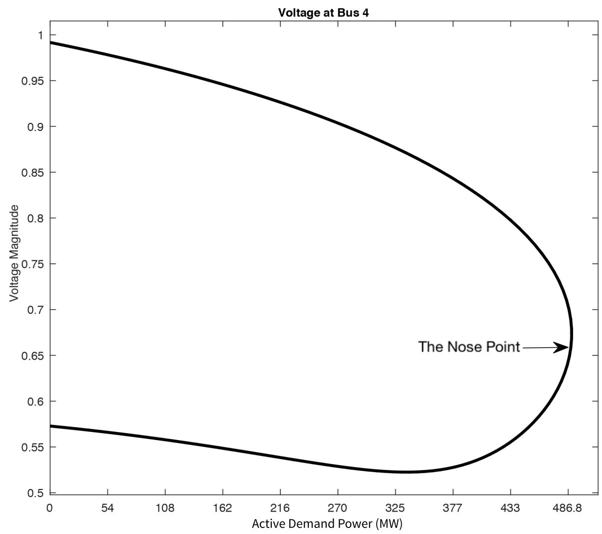

Fig. 6. PV Curve of Bus 4

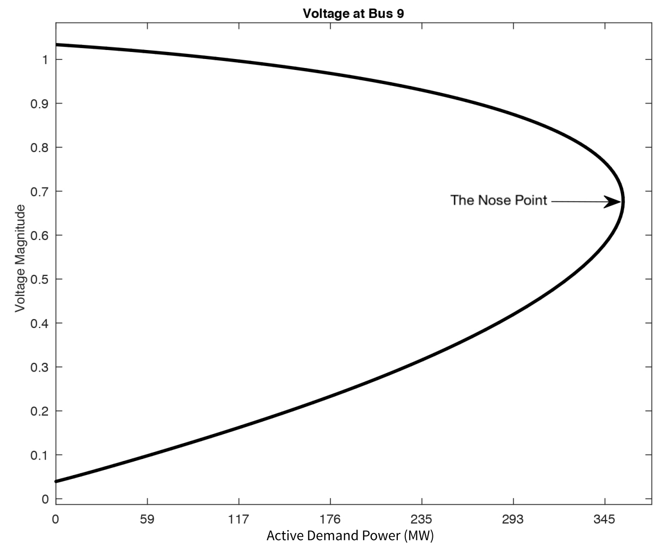

Fig. 7. The PV curve of bus 9

TABLE XIII
14-BUS SYSTEM MAXIMUM LOADING LEVEL

Bus	$\|V\|$(p.u.)	δ (degrees)	P_D(MW)	Compensation
Bus 4	0.6766	-81.0280	715.7236	Q_{G4} = 0 MVAr
Bus 5	0.6754	-71.9308	682.4810	Q_{G5} = 0 MVAr
Bus 7	0.7530	-88.7925	353.3889	Q_{G7} = 0 MVAr
Bus 10	0.6440	-79.6868	253.2913	Q_{G10} = 0 MVAr
Bus 11	0.6361	88.9029	251.2200	Q_{G11} = 0 MVAr
Bus 12	0.6014	86.4068	206.7138	Q_{G12} = 0 MVAr
Bus 13	0.7246	61.9912	314.0533	Q_{G13} = 0 MVAr
Bus 14	0.6164	-67.9183	160.4554	Q_{G14} = 0 MVAr
Bus 9	0.6733	-86.7417	351.7682	Q_{G9} = 0 MVAr
Bus 9	0.6885	-89.3901	363.6388	Q_{G9} = 19 MVAr
Bus 9	0.6974	89.1735	370.1267	Q_{G9} = 30 MVAr
Bus 9	0.7139	86.7336	381.2615	Q_{G9} = 50 MVAr
Bus 9	0.7560	81.5239	405.8269	Q_{G9} = 100 MVAr
Bus 9	0.7990	77.4211	426.5157	Q_{G9} = 150 MVAr
Bus 9	0.8422	74.2203	444.1128	Q_{G9} = 200 MVAr

convex relaxation of AC OPF problem when the system is operating at the physical constraint limits.

Further, we introduced identifying the maximum power loading level. We show that the results from SDP OPF well match the results obtained from MATPOWER's CPF method.

REFERENCES

[1] X. Bai, H. Wei, K. Fujisawa, and Y. Wang, "Semidefinite programming for optimal power flow problems," *International Journal of Electrical Power & Energy Systems*, vol. 30, no. 6, pp. 383–392, 2008.

[2] J. Lavaei and S. H. Low, "Zero duality gap in optimal power flow problem," *IEEE Transactions on Power Systems*, vol. 27, no. 1, pp. 92–107, 2012.

[3] R. D. Zimmerman, C. E. Murillo-Sánchez, and R. J. Thomas, "Matpower: Steady-state operations, planning, and analysis tools for power systems research and education," *IEEE Transactions on power systems*, vol. 26, no. 1, pp. 12–19, 2011.

[4] D. K. Molzahn, B. C. Lesieutre, and C. L. DeMarco, "A sufficient condition for power flow insolvability with applications to voltage stability margins," *IEEE Transactions on Power Systems*, vol. 28, no. 3, pp. 2592–2601, Aug 2013.

[5] D. K. Molzahn, I. A. Hiskens, and B. C. Lesieutre, "Calculation of voltage stability margins and certification of power flow insolvability using second-order cone programming," in *System Sciences (HICSS), 2016 49th Hawaii International Conference on*. IEEE, 2016, pp. 2307–2316.

[6] J. A. Momoh, *Electric power system applications of optimization*. CRC Press, 2008.

[7] D. K. Molzahn, S. S. Baghsorkhi, and I. A. Hiskens, "Semidefinite relaxations of equivalent optimal power flow problems: An illustrative example," in *Circuits and Systems (ISCAS), 2015 IEEE International Symposium on*. IEEE, 2015, pp. 1887–1890.

[8] M. Grant, S. Boyd, and Y. Ye, "Cvx: Matlab software for disciplined convex programming," 2008.

[9] S. Sojoudi, R. Madani, and J. Lavaei, "Low-rank solution of convex relaxation for optimal power flow problem," in *Smart Grid Communications (SmartGridComm), 2013 IEEE International Conference on*. IEEE, 2013, pp. 636–641.

[10] A. J. Wood and B. Wollenberg, "Power generation operation and control, 2nd edition," in *Fuel and Energy Abstracts*, vol. 37, no. 3. Elsevier, 1996, p. 195.

[11] "Power systems test case archive, university of washington," *http://www.ee.washington.edu/research/pstca*.

[12] L. Fan, *Control and Dynamics in Power Systems and Microgrids*. CRC Press, 2017.